

# Modified Oligonucleotides Containing Lithocholic Acid in Their Backbones: Their Enhanced Cellular Uptake and Their Mimicking of Hairpin Structures

Su Jeong Kim,<sup>[a]</sup> Eun-Kyoung Bang,<sup>[a]</sup> Ho Jeong Kwon,<sup>[b]</sup> Joong Sup Shim,<sup>[b]</sup> and Byeang Hyeon Kim\*<sup>[a]</sup>

*Their enhanced cell permeability and their ability to mimic DNA structures make modified oligodeoxyribonucleotides (ODNs) very important substances for increasing our understanding of cell biology and for therapeutic applications. Lithocholic acid is a hydrophobic secondary bile acid that is a substrate of nuclear Pregnane X receptor (PXR). We designed and synthesized novel lithocholic acid-based ODNs (L-ODNs) by using a new phosphoramidite derived from lithocholic acid. By comparing data obtained*

*from circular-dichroism, melting-point, and theoretical studies, we believe that these L-ODNs adopt DNA hairpin structures. Furthermore, L-ODNs have enhanced cellular uptake properties with respect to regular ODNs. To demonstrate their enhanced cell permeabilities, we carried out cellular uptake experiments of L-ODNs in HeLa cells. By attaching fluorescein as a fluorescence label and using confocal microscopy, we observed that the permeability of L-ODNs is much higher than that of natural ODNs.*

## Introduction

In recent years the study of modified oligodeoxyribonucleotides (ODNs) has become an area of increased research activity.<sup>[1]</sup> The synthesis of modified ODNs provides research opportunities for preparing 1) therapeutic reagents, by regulating gene and protein expression through antisense and antigene strategies,<sup>[2]</sup> 2) diagnostic agents, by sequencing genomes and identifying genetic abnormalities,<sup>[3]</sup> 3) probes, by detecting DNA–DNA, DNA–RNA, and DNA–protein interactions,<sup>[4]</sup> and 4) molecular architectures, by base-pairing between programmed sequences.<sup>[5]</sup> The specific applications of each phosphoramidite molecule used for preparing new modified ODNs are dictated by its chemical and physical properties. We were interested in using lithocholic acid, which is a hydrophobic secondary bile acid and a substrate of nuclear Pregnane X receptor (PXR), as a unit within ODNs.<sup>[6]</sup> Because lithocholic acid has one carboxyl group and one secondary hydroxyl group, it can be adapted to the general protocols of ODN synthesis by using the phosphoramidite method. Cholesterol is known for its ability to penetrate and interact with cell membranes.<sup>[7]</sup> In most cases, cholesterol molecules have been linked at the 3' or 5' terminus of ODNs, whereas we chose to insert the molecule in the middle of the chain. We expect that ODNs incorporating a cholane-3,24-diol ( $3\alpha,5\beta$ )<sup>[8]</sup> unit, which is a reduced form of lithocholic acid, could exhibit relatively enhanced cellular uptake properties because of the presence of this cholesterol-like unit. Additionally, cholane-3,24-diol ( $3\alpha,5\beta$ ) meets the general criteria for modification of ODNs<sup>[9]</sup> and it can be used as a platform for hairpin-type ODNs (Figure 1).<sup>[10]</sup> Indeed, molecular modeling studies on a simple modified ODN (5'-d-AALTT) resulted in a hairpin-type ODN (Figure 2).<sup>[11]</sup> In this paper, we de-

scribe the synthesis and characterization of a novel phosphoramidite monomer formed using lithocholic acid and its incorporation into ODNs. We have studied the behavior of these modified ODNs as hairpin mimics by analysis of data from melting point ( $T_m$ ), CD spectroscopic, and cell-based permeability studies.

## Results and Discussion

### Synthesis of phosphoramidite **4** and L-ODNs

We synthesized cholane-3,24-diol ( $3\alpha,5\beta$ ) (**2**) readily by reduction of the carboxyl group of lithocholic acid (**1**) (Scheme 1). The primary hydroxyl group of cholane-3,24-diol ( $3\alpha,5\beta$ ) was protected selectively by using the 4,4'-dimethoxytrityl (DMTr) group. The desired phosphoramidite **4** was obtained by coupling the secondary hydroxyl group of 24-O-(4,4'-dimethoxytrityloxy)cholane-3,24-diol (**3**) with chloro-(2-cyanoethoxy)-N,N-

[a] Dr. S. J. Kim, E.-K. Bang, Prof. Dr. B. H. Kim  
Department of Chemistry, Division of Molecular and Life Sciences  
Pohang University of Science and Technology  
San 31 Hyoja Dong, Pohang 790-784 (Korea)  
Fax: (+82) 54-279-3399  
E-mail: bhkim@postech.ac.kr

[b] Prof. Dr. H. J. Kwon, J. S. Shim  
Department of Bioscience and Biotechnology, Institute of Bioscience  
Sejong University, Seoul 143-747 (Korea)

Supporting information for this article is available on the WWW under <http://www.chembiochem.org> or from the author.

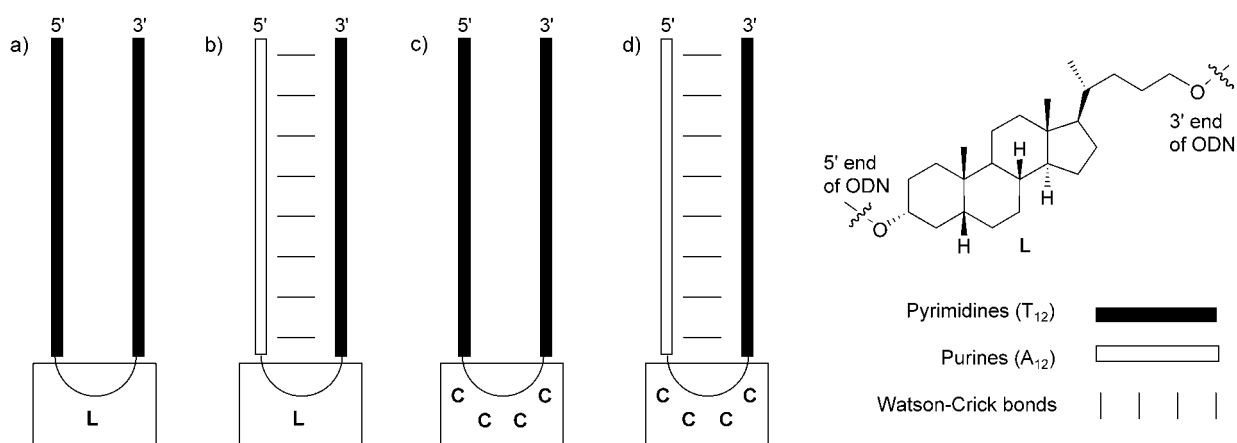


**Figure 1.** Possible structures of  $T_{12}$ -L- $T_{12}$ ,  $A_{12}$ -L- $T_{12}$ ,  $T_{12}$ -C<sub>4</sub>- $T_{12}$ , and  $A_{12}$ -C<sub>4</sub>- $T_{12}$ : a)  $T_{12}$ -L- $T_{12}$ : random coil. b)  $A_{12}$ -L- $T_{12}$ : hairpin mimic. c)  $T_{12}$ -C<sub>4</sub>- $T_{12}$ : random coil. d)  $A_{12}$ -C<sub>4</sub>- $T_{12}$ : natural hairpin structure. The cholane-3,24-diol ( $3\alpha,5\beta$ ) unit is denoted by the letter L.

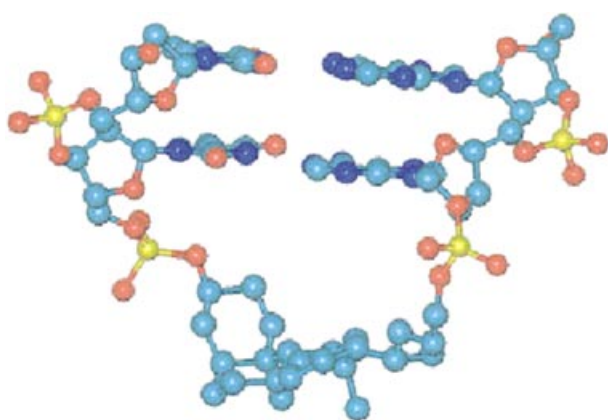
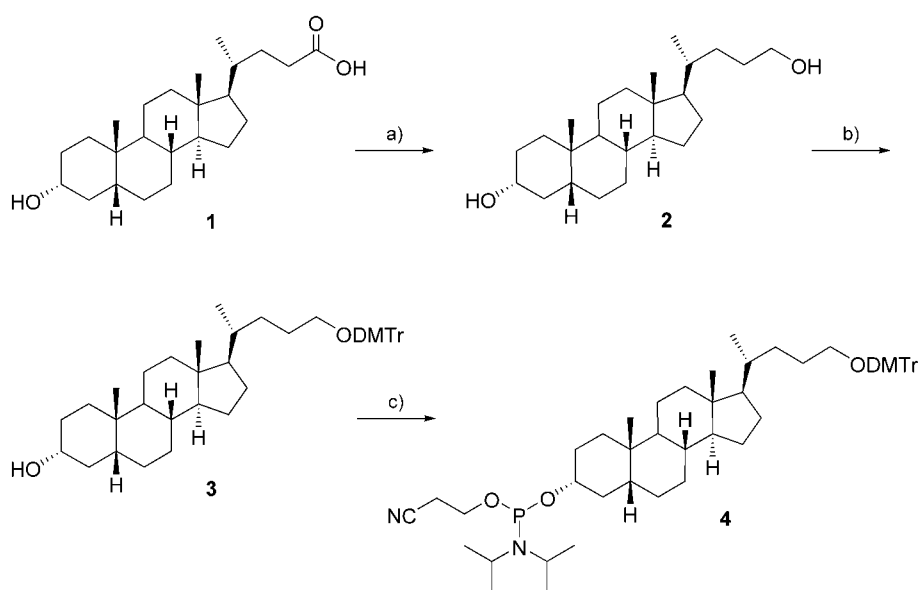


**Figure 2.** Optimized structure of a simple L-ODN (sequence: 5'-d-AALTT). Local energy-minimized structure obtained by the MM+ force-field method.

diisopropylaminophosphine. The overall yield for the three steps was 46%.

The novel phosphoramidite **4** was applied successfully to the synthesis of lithocholic acid-based ODNs. We designed the modified ODNs (L-ODNs) with a cholane-3,24-diol ( $3\alpha,5\beta$ ) unit in the middle of their ODN sequences so that they would be mimics of hairpin structures, and we synthesized them using the protocols of solid-phase oligonucleotide synthesis<sup>[12]</sup> on an automated DNA synthesizer (PerSeptive Biosystems 8909 Expedite™ Nucleic Acid Synthesis System). For comparison, the unmodified ODNs were also prepared. We confirmed that the syntheses of these L-ODNs were successful by DMTr monitoring (see Supporting Information). The modified ODNs were purified by reversed-phase HPLC. These modified ODNs were characterized by MALDI-TOF mass spectrometry (Table 1).



**Scheme 1.** Synthesis of phosphoramidite derivative **4**. a)  $\text{LiAlH}_4$  (4.6 equiv), THF, 4 h, 96%. b) DMTrCl (1.9 equiv), DMAP, Et<sub>3</sub>N, pyridine, 89%. c) Chloro-(2-cyanoethoxy)-N,N-diisopropylaminophosphine (1.5 equiv), DIPEA (3 equiv),  $\text{CH}_2\text{Cl}_2$ , 54%.

### UV spectroscopic melting experiments: Structural studies of L-ODNs as hairpin mimics

We analyzed the binding affinities of L-ODNs by obtaining UV spectroscopic melting curves, with melting transitions monitored at both 260 and 284 nm. The UV spectral absorbance of the A-T Watson-Crick duplexes did not appear to change when their melting transitions were monitored at 284 nm, since this wavelength marks an isosbestic point of double-helix structures with A-T-rich sequences.<sup>[13]</sup> Thus, any change in the absorbance at 284 nm is induced by structural transitions other than simple duplex formation/destruction, such as triplex or more complex aggregations. Table 2 summarizes

**Table 1.** MALDI-TOF mass spectroscopic data of the L-ODNs.

Sequence	Calculated	Found
5'-d-T <sub>12</sub> -L-T <sub>12</sub>	7663.3	7662.7
5'-d-A <sub>12</sub> -L-T <sub>12</sub>	7771.5	7771.5
5'-d-AACGTT L AACGTT	4069.0	4067.8
5'-d-CAACGTT L AACGTTG	4687.4	4689.2
5'-d-CCAACGTT L AACGTTGG	5305.8	5304.8

Conditions: PE Biosystems Voyager System 4095, accelerating voltage: 20000 V, matrix: 2,5-dihydroxybenzoic acid, polarity: positive.

**Table 2.** Melting temperatures of synthetic L-ODNs.

Name	Sequences	T <sub>m</sub> (260 nm)	T <sub>m</sub> (284 nm)
1	T <sub>12</sub> -L-T <sub>12</sub> 5'-d-T <sub>12</sub> LT <sub>12</sub>	No T <sub>m</sub>	No T <sub>m</sub>
2	A <sub>12</sub> -L-T <sub>12</sub> 5'-d-A <sub>12</sub> LT <sub>12</sub>	74 °C	No T <sub>m</sub>
3	T <sub>12</sub> -C <sub>4</sub> -T <sub>12</sub> 5'-d-T <sub>12</sub> C <sub>4</sub> T <sub>12</sub>	No T <sub>m</sub>	No T <sub>m</sub>
4	A <sub>12</sub> -C <sub>4</sub> -T <sub>12</sub> 5'-d-A <sub>12</sub> C <sub>4</sub> T <sub>12</sub>	68 °C	29 °C <sup>[a]</sup>
5	X <sub>6</sub> -C <sub>4</sub> -X <sub>6</sub> 5'-d-AACGTT C <sub>4</sub> AACGTT	66 °C	n.d. <sup>[b]</sup>
6	X <sub>6</sub> -L-X <sub>6</sub> 5'-d-AACGTT LAACGTT	72 °C	n.d. <sup>[b]</sup>
7	X <sub>7</sub> -L-X <sub>7</sub> 5'-d-CAACGTT LAACGTTG	76 °C	n.d. <sup>[b]</sup>
8	X <sub>8</sub> -L-X <sub>8</sub> 5'-d-CCAACGTT LAACGTTGG	82 °C	n.d. <sup>[b]</sup>
9	A <sub>12</sub> /T <sub>12</sub> 5'-d-A <sub>12</sub> /5'-d-T <sub>12</sub>	38 °C	No T <sub>m</sub>
10	T <sub>12</sub> -L-T <sub>12</sub> /A <sub>12</sub> 5'-d-T <sub>12</sub> LT <sub>12</sub> /5'-d-A <sub>12</sub>	55 °C	55 °C
11	T <sub>12</sub> -C <sub>4</sub> -T <sub>12</sub> /A <sub>12</sub> 5'-d-T <sub>12</sub> C <sub>4</sub> T <sub>12</sub> /5'-d-A <sub>12</sub>	53 °C	53 °C
12	A <sub>12</sub> -L-T <sub>12</sub> /T <sub>12</sub> 5'-d-A <sub>12</sub> LT <sub>12</sub> /5'-d-T <sub>12</sub>	17, 75 °C	17 °C
13	A <sub>12</sub> -C <sub>4</sub> -T <sub>12</sub> /T <sub>12</sub> 5'-d-A <sub>12</sub> C <sub>4</sub> T <sub>12</sub> /5'-d-T <sub>12</sub>	19, 70 °C	19 °C

Values of T<sub>m</sub> were determined by measuring changes in absorbance at 260 and 284 nm (cuvette, 1 cm path length) as a function of temperature in Tris-HCl buffer (10 mM, pH 7.2) containing NaCl (100 mM) and MgCl<sub>2</sub> (20 mM). The temperature was raised at a rate of 1.0 °C min<sup>-1</sup>. Total ODN concentration is 3 μM. [a] T<sub>m</sub> value measured at 284 nm is induced by the C<sub>4</sub> units, since 284 nm is not an isosbestic point for the cytidine base. [b] n.d. = not detected.

es the sequences of the ODNs and the data from their thermal denaturing experiments. Figure 3 displays the relative absorbance of curves used for determining values of T<sub>m</sub>. Entries 1 and 3 suggest that T<sub>12</sub>-L-T<sub>12</sub> and T<sub>12</sub>-C<sub>4</sub>-T<sub>12</sub> do not have double-helix geometries. T<sub>12</sub>-L-T<sub>12</sub>, which has a unit of compound 4 incorporated into the middle of a dT<sub>24</sub> sequence, cannot adopt a double-stranded secondary structure (entry 1). Similarly, T<sub>12</sub>-C<sub>4</sub>-T<sub>12</sub>, which has a C<sub>4</sub> hairpin-loop unit incorporated into the middle of the dT<sub>24</sub> sequence, cannot adopt a double-stranded secondary structure either (entry 3). Thus, the structures of T<sub>12</sub>-L-T<sub>12</sub> and T<sub>12</sub>-C<sub>4</sub>-T<sub>12</sub> must be random coils, a situation that is confirmed by the lack of measurable values of T<sub>m</sub> at both 260 and 284 nm.<sup>[14]</sup> A<sub>12</sub>-L-T<sub>12</sub>, which incorporates a unit of compound 4 in the middle of a dA<sub>12</sub>T<sub>12</sub> sequence, has a T<sub>m</sub> value of 74 °C when detected at 260 nm, but does not have an observable value of T<sub>m</sub> when measured at 284 nm. Thus, A<sub>12</sub>-L-T<sub>12</sub> appears to adopt a double-stranded secondary structure (entry 2). A<sub>12</sub>-C<sub>4</sub>-T<sub>12</sub>, which incorporates a C<sub>4</sub> unit (a natural hairpin domain) into the middle of the dA<sub>12</sub>T<sub>12</sub> sequence, almost certainly adopts a secondary structure<sup>[15]</sup> (hairpin structure; entry 4) and has a high value of T<sub>m</sub>. We observed the same results in the cases of hairpins containing hetero-sequences (en-

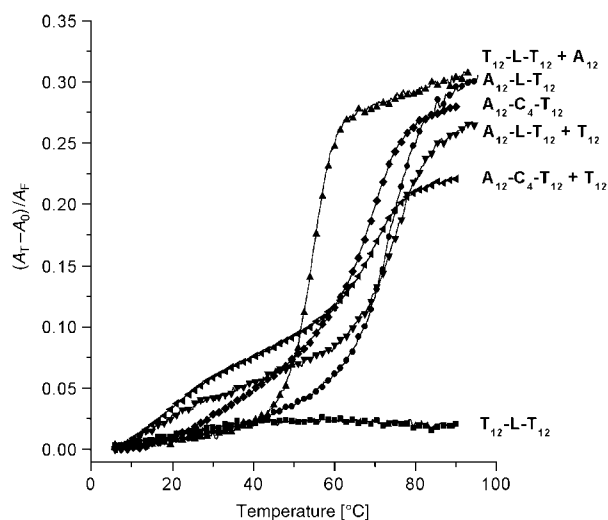


**Figure 3.** Thermal denaturation curves of synthetic ODNs at 260 nm. All absorbance data are normalized ( $A_T$ : absorbance at temperature  $T$ ;  $A_0$ : absorbance at initial temperature;  $A_f$ : absorbance at final temperature).

tries 5–8). X<sub>6</sub>-C<sub>4</sub>-X<sub>6</sub>, which has a C<sub>4</sub> hairpin-loop unit incorporated into the middle of an inverted repeat sequence (palindrome), forms a hairpin structure (entry 5). X<sub>6</sub>-L-X<sub>6</sub> possibly forms a hairpin structure that is more stable than the natural sequence (entry 6). As the length of the palindrome was increased, the stability of the hairpin structure also increased (entries 6–8). We did not measure at 284 nm because this wavelength is not an isosbestic point of these hetero-sequences (entries 5–8). Over a 40-fold concentration range, the T<sub>m</sub> values of A<sub>12</sub>-L-T<sub>12</sub> and X<sub>6</sub>-L-X<sub>6</sub> do not depend on the strand concentration; this confirms the formation of the intramolecular hairpin structures (see Supporting Information).

To investigate triplex formation, we determined the values of T<sub>m</sub> for a mixture of ODNs. The mixtures of T<sub>12</sub>-L-T<sub>12</sub> and A<sub>12</sub> (entry 10) and T<sub>12</sub>-C<sub>4</sub>-T<sub>12</sub> and A<sub>12</sub> (entry 11) each have one value of T<sub>m</sub> of 55 °C when measured at both 260 and 284 nm. Presumably, one dT<sub>12</sub> sequence of T<sub>12</sub>-L-T<sub>12</sub> (or T<sub>12</sub>-C<sub>4</sub>-T<sub>12</sub>) forms a double helix with the added dA<sub>12</sub> and then the other dT<sub>12</sub> sequence of T<sub>12</sub>-L-T<sub>12</sub> (or T<sub>12</sub>-C<sub>4</sub>-T<sub>12</sub>) assembles with it to form a triplex. The duplex and triplex must dissociate simultaneously because only one value of T<sub>m</sub> was observed. Both the mixture of A<sub>12</sub>-L-T<sub>12</sub> and T<sub>12</sub> (entry 12) and the mixture of A<sub>12</sub>-C<sub>4</sub>-T<sub>12</sub> and T<sub>12</sub> (entry 13) have two values of T<sub>m</sub>. The dT<sub>12</sub> and dA<sub>12</sub> sequences of A<sub>12</sub>-L-T<sub>12</sub> (or A<sub>12</sub>-C<sub>4</sub>-T<sub>12</sub>) assemble into a double helix (having a hairpin structure) through intramolecular Watson-Crick base pairing, and then the added dT<sub>12</sub> unit (T<sub>12</sub>) forms a triplex with it through Hoogsteen base-pairing. Thus, A<sub>12</sub>-L-T<sub>12</sub> and A<sub>12</sub>-C<sub>4</sub>-T<sub>12</sub> appear to form similar double- and triple-stranded assemblies when a complementary third strand is added to each of them and, hence, the L-ODN structure can be used a substitute building block for hairpin loops.

### CD spectroscopic studies

CD spectroscopy is a useful method for distinguishing the structures of ODNs.<sup>[16]</sup> We have applied this technique to study

the conformational changes arising from the modification of the ODNs. In Figure 4a, we display superimposed CD spectra of the modified and natural ODNs. The CD spectra of  $T_{12}$ -L- $T_{12}$  and  $T_{12}$ -C<sub>4</sub>- $T_{12}$  each have weak positive CD bands at 218 and 281 nm and a weak negative CD band at 248 nm. This pattern is almost the same as that displayed by  $T_{12}$ . The CD spectra of  $A_{12}$ -L- $T_{12}$  and  $A_{12}$ -C<sub>4</sub>- $T_{12}$  each have positive CD bands at 218 and 283 nm and a negative CD band at 249 nm. These CD spectra are almost identical to that of the mixture of  $A_{12}$  and  $T_{12}$ ; this indicates that they might possess B-form duplex structures. In Figure 4b, the CD spectra representing the formation of triplexes are superimposed. The CD spectrum of  $T_{12}$ -L- $T_{12}$ : $A_{12}$  has strong positive CD bands at 217 and 281 nm and negative CD bands at 207 and 248 nm. The CD spectrum of  $T_{12}$ -L- $T_{12}$  alone reflects its random coil structure (Figure 4a, ■). The CD spectrum of  $T_{12}$ -L- $T_{12}$  in the presence of  $A_{12}$ , however, is changed dramatically to have almost the same pattern as the spectrum of the mixture between  $A_{12}$ -C<sub>4</sub>- $T_{12}$  and  $T_{12}$ . This observation suggests that the mixture of  $T_{12}$ -L- $T_{12}$  and  $A_{12}$  adopts a triplex structure similar to the one formed by  $A_{12}$ -C<sub>4</sub>- $T_{12}$ : $T_{12}$ . Thus, these circular dichroism spectra suggest that the L-ODNs do indeed adopt DNA-hairpin structures.

#### Studying cellular uptake and stability to the nuclease

To analyze the cell permeability of synthetic ODNs, we attached FITC (fluorescein) as a fluorescence label at the 5' ends of  $T_{12}$ -L- $T_{12}$  and  $T_{12}$ -C<sub>4</sub>- $T_{12}$ . We studied the uptake of these ODNs in HeLa cells (Figure 5). We used two commercially available fluorescence dyes, DAPI (blue) and MitoTracker Red (red), to detect the cellular localization of the nucleus and mitochondria, respectively. From the confocal microscopy images, we observe that the permeability of  $T_{12}$ -L- $T_{12}$ -FITC is much higher

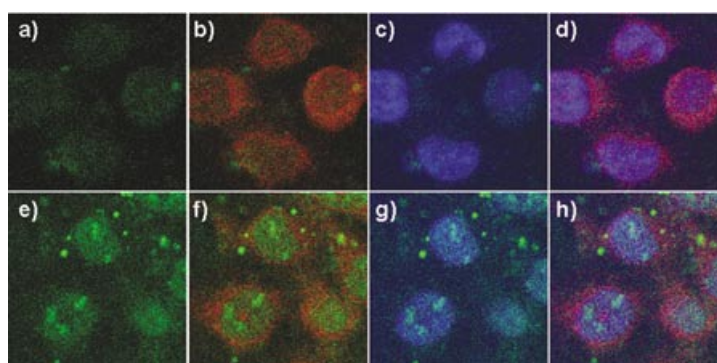


**Figure 5.** Confocal microscopic images of synthetic ODNs. a)  $T_{12}$ -C<sub>4</sub>- $T_{12}$ -FITC. b)  $T_{12}$ -C<sub>4</sub>- $T_{12}$ -FITC and MitoTracker Red (merged image). c)  $T_{12}$ -C<sub>4</sub>- $T_{12}$ -FITC and DAPI (merged image). d)  $T_{12}$ -C<sub>4</sub>- $T_{12}$ -FITC, DAPI, and MitoTracker Red (merged image). e)  $T_{12}$ -L- $T_{12}$ -FITC. f)  $T_{12}$ -L- $T_{12}$ -FITC and MitoTracker Red; bar: 10  $\mu$ m (merged image). g)  $T_{12}$ -L- $T_{12}$ -FITC and DAPI (merged image). h)  $T_{12}$ -L- $T_{12}$ -FITC, DAPI, and MitoTracker Red (merged image). Incubation time: 10 h.

than that of  $T_{12}$ -C<sub>4</sub>- $T_{12}$ -FITC and that  $T_{12}$ -L- $T_{12}$ -FITC localizes mainly at the nucleus; this is consistent with the fact that L is a substrate of the nuclear receptor. The uptake level of  $T_{12}$ -C<sub>4</sub>- $T_{12}$ -FITC is the basal-level uptake of the oligonucleotides by cells.<sup>[7e]</sup> At present, we do not know the exact mechanism of the nuclear localization. The dye FITC is known to bleach out very quickly during confocal imaging in the cell, and, therefore, we measured such images at a variety of times (Figure 6). After incubation for 15 min, we observed that the sample treated with  $T_{12}$ -L- $T_{12}$ -FITC had a higher number of cells that displayed green emission than did the sample treated with  $T_{12}$ -C<sub>4</sub>- $T_{12}$ -FITC. The highest permeation efficiency of  $T_{12}$ -L- $T_{12}$ -FITC was observed after incubation for 8 h. Longer incubation times (> 15 h), however, cause intensities to decrease, possibly because of degradation by cellular nucleases. Consistent with this observation,  $T_{12}$ -L- $T_{12}$ -FITC and  $T_{12}$ -C<sub>4</sub>- $T_{12}$ -FITC degrade in vitro in the presence of DNase I in a manner similar to that of a control unmodified ODN (see Supporting Information).

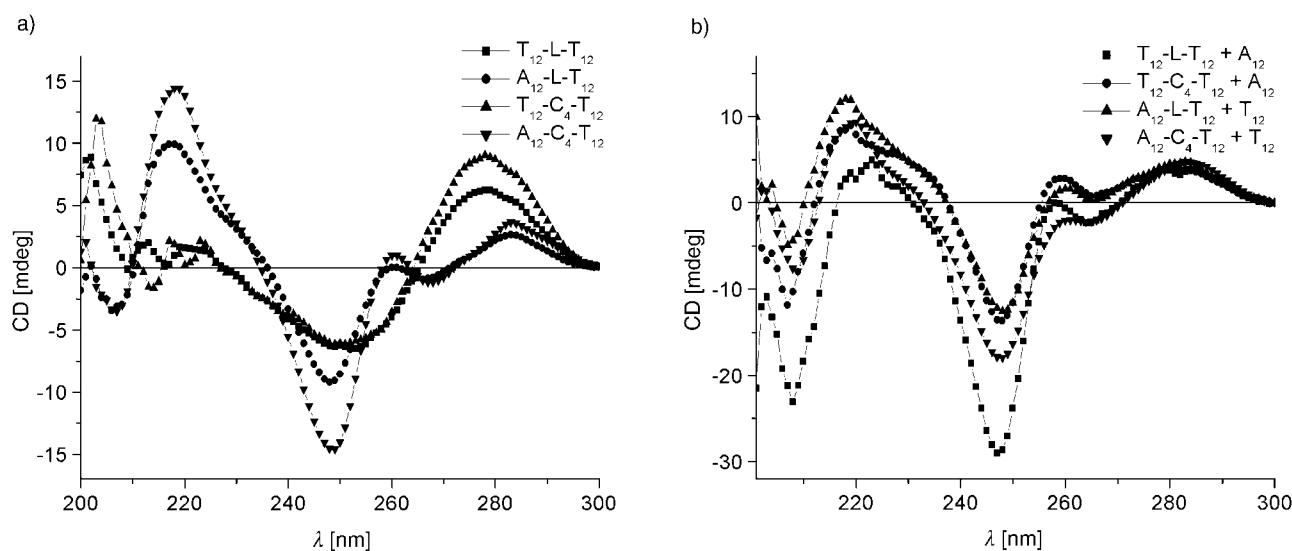


**Figure 4.** CD spectra of synthesized ODNs. All curves were obtained at 10 °C. a)  $T_{12}$ -L- $T_{12}$  (■);  $A_{12}$ -L- $T_{12}$  (●);  $T_{12}$ -C<sub>4</sub>- $T_{12}$  (▲);  $A_{12}$ -C<sub>4</sub>- $T_{12}$  (▼). b) A mixture of  $T_{12}$ -L- $T_{12}$  and  $A_{12}$  (■); a mixture of  $T_{12}$ -C<sub>4</sub>- $T_{12}$  and  $A_{12}$  (●); a mixture of  $A_{12}$ -L- $T_{12}$  and  $T_{12}$  (▲); a mixture of  $A_{12}$ -C<sub>4</sub>- $T_{12}$  and  $T_{12}$  (▼). The experimental conditions are described in Table 2.

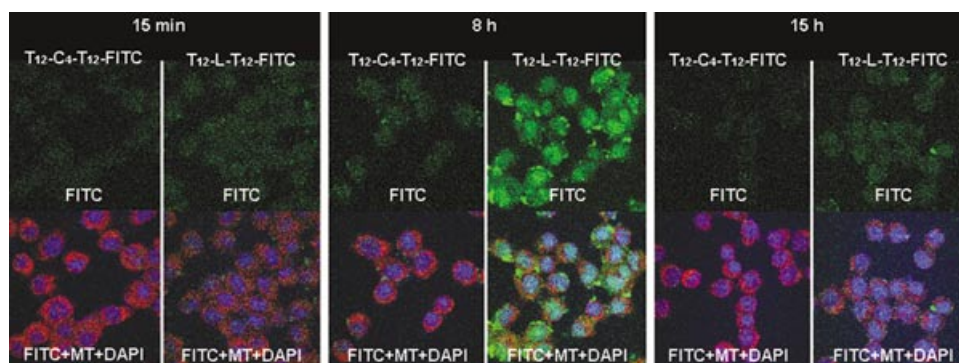


Figure 6. Incubation-time-dependent confocal microscopic images of synthetic ODNs.

## Conclusion

We have designed and synthesized a novel phosphoramidite monomer from lithocholic acid and have incorporated it into ODNs as a structural scaffold for preparing hairpin mimics. The secondary structures of L-ODNs were confirmed by determining values of  $T_m$  and by analyzing CD spectra. These analyses revealed that the L-ODNs adopt hairpin structures with double-helix formation through intramolecular hydrogen bonding between complementary sequences of ODNs, that is, they mimic natural DNA hairpin structures. These ODNs can adopt triplex structures when they assemble with an added third strand. We also investigated whether incorporation of cholane-3,24-diol ( $3\alpha,5\beta$ ) into L-ODNs provides an enhancement in their cellular uptake by penetrating and interacting with cell membranes and nuclei. The L scaffold serves a double purpose: to mediate the formation of a stable hairpin structure and to increase cell permeability. Currently, we are preparing L-ODNs that contain hetero-sequences and mismatched sequences for similar studies.

## Experimental Section

**Instruments and methods:** All solvents were dried and distilled carefully prior to use.  $^1\text{H}$  NMR and  $^{13}\text{C}$  NMR spectra were obtained on an FT-300 MHz Bruker Aspect 3000 spectrometer. Mass spectra (FAB) were obtained by using a Jeol JMS-AX505WA spectrometer at the Korea Basic Science Center, Daejeon, Korea. The IR spectra were obtained on a Bruker FTIR P555+ spectrometer. Values of  $T_m$  were determined by using a Shimadzu UV-2501PC UV/Vis spectrophotometer; the temperature was adjusted by a Polyscience 9110 programmable digital temperature controller. The mixture of ODNs was equilibrated by cooling it to  $5^\circ\text{C}$ , then, after 30 min, the CD spectra were recorded on a Jasco J-715 CD-spectropolarimeter. The temperature was adjusted by using a Jasco PTC-348WI temperature controller. All reactions were performed in oven-dried glassware under a positive pressure of argon. Analytical TLC was performed on precoated silica gel plates and visualized with UV light and/or by spraying with *p*-anisaldehyde or phosphomolybdic acid solutions followed by heating on a hotplate. Flash column chromatography was performed with silica gel.

**Cholane-3,24-diol ( $3\alpha,5\beta$ ) (2):**  $\text{LiAlH}_4$  (248 mg, 6.58 mmol) was added slowly to a solution of lithocholic acid (**1**; 527 mg, 1.40 mmol) in anhydrous THF (30 mL) at  $0^\circ\text{C}$ . The reaction mixture

was then stirred for 2.5 h at room temperature.  $\text{H}_2\text{O}$  (250  $\mu\text{L}$ ), 15% aqueous NaOH (250  $\mu\text{L}$ ), and more  $\text{H}_2\text{O}$  (750  $\mu\text{L}$ ) were added sequentially to the reaction mixture. The white solid was removed by filtration. The organic layer was dried ( $\text{MgSO}_4$ ) and concentrated under reduced pressure. Purification by flash chromatography gave the product (486 mg, 1.33 mmol, 95%) as a white solid. M.p.  $96.5\text{--}97.8^\circ\text{C}$ ;  $^1\text{H}$  NMR (300 MHz,  $\text{CDCl}_3$ )  $\delta = 3.61\text{--}3.57$  (m, 3 H),  $1.82\text{--}1.01$  (m, 28 H),  $0.90$  (s, 6 H),  $0.62$  (s, 3 H);  $^{13}\text{C}$  NMR (75.5 MHz,  $\text{CDCl}_3$ )  $\delta = 70.3, 62.0, 56.0, 55.7, 42.1, 41.6, 35.9, 35.3,$

$35.1, 35.0, 34.1, 31.5, 30.0, 29.0, 27.8, 26.8, 26.0, 23.7, 23.0, 20.3, 18.2, 11.6$ ; IR (neat):  $\tilde{\nu} = 3205, 2934, 2862, 1446, 1066, 914, 728\text{ cm}^{-1}$ ; HRMS (FAB): calcd for  $\text{C}_{24}\text{H}_{41}\text{O}$ : 345.3157 [ $\text{M}-\text{OH}$ ] $^+$ ; found 345.20; Crystal data ( $\text{C}_{24}\text{H}_{42}\text{O}_2 + \text{CH}_2\text{Cl}_2$ ):  $M_r = 447.50$ , orthorhombic, space group  $P2(1)2(1)2(1)$ ,  $a = 7.3920(12)$ ,  $b = 16.088(3)$ ,  $c = 21.568(4)\text{ \AA}$ ,  $\alpha = 90.0000$ ,  $\beta = 90.0000$ ,  $\gamma = 90.0000^\circ$ ,  $V = 2565.0(7)\text{ \AA}^3$ ,  $Z = 4$ ,  $\rho_{\text{calcd}} = 1.159\text{ Mg m}^{-3}$ ,  $\text{MoK}\alpha$  radiation ( $\lambda = 0.71073\text{ \AA}$ ). Of 11 410 reflections collected on a Siemens SMART diffractometer equipped with a CCD detector, 3692 were observed ( $R_{\text{int}} = 0.1685$ ) and used for all calculations (program: SHELXL-97). After absorption correction (psi scans) the structure was solved by direct methods and refined anisotropically on  $F^2$ . Final residuals:  $R_1 = 0.0828$ ,  $wR_2 = 0.2321$  ( $I > 2\sigma(I)$ );  $R_1 = 0.0963$ ,  $wR_2 = 0.2471$  (all data), 268 parameters.

CCDC-210019 contains the supplementary crystallographic data for this paper. These data can be obtained free of charge via [www.ccdc.cam.ac.uk/conts/retrieving.html](http://www.ccdc.cam.ac.uk/conts/retrieving.html) (or from the Cambridge Crystallographic Data Centre, 12 Union Road, Cambridge CB2 1EZ, UK; fax: (+44) 1223-336033; or [deposit@ccdc.cam.ac.uk](mailto:deposit@ccdc.cam.ac.uk)).

**24-O-(4,4'-Dimethoxytrityloxy)cholane-3,24-diol ( $3\alpha,5\beta$ ) (3):** DMTr-Cl (544 mg, 1.63 mmol) was added to a solution of cholane-3,24-diol ( $3\alpha,5\beta$ ) (**2**; 455 mg, 1.25 mmol) and DMAP (68 mg, 0.56 mmol) in pyridine (10 mL). The reaction mixture was stirred at room temperature for 19 h, and then the solvent was evaporated under reduced pressure. Distilled  $\text{H}_2\text{O}$  (90 mL) and EtOAc (30 mL) were added. The organic layer was dried ( $\text{MgSO}_4$ ) and concentrated under reduced pressure. Purification by flash chromatography (EtOAc/hexane 1:4) provided the product (744 mg, 1.12 mmol, 89%) as a white solid. M.p.  $81.2\text{--}82.1^\circ\text{C}$ ;  $^1\text{H}$  NMR (300 MHz,  $\text{CDCl}_3$ )  $\delta = 7.45$  (d,  $J = 7.2\text{ Hz}$ , 2H),  $7.35\text{--}7.26$  (m, 7H),  $6.89\text{--}6.80$  (dd,  $J_1 = 7.0$ ,  $J_2 = 1.9\text{ Hz}$ , 4H),  $3.80$  (s, 6H),  $3.64$  (br, 1H),  $3.04\text{--}2.98$  (m, 2H),  $1.99\text{--}0.89$  (m, 34H),  $0.63$  (s, 3H);  $^{13}\text{C}$  NMR (75.5 MHz,  $\text{CDCl}_3$ ):  $\delta = 159.0, 148.2, 137.6, 130.7, 129.0, 128.3, 127.2, 126.6, 113.7, 86.4, 72.6, 64.7, 57.3, 56.9, 55.9, 43.4, 42.9, 41.2, 40.9, 37.2, 36.6, 36.3, 36.1, 35.3, 33.1, 31.3, 28.9, 27.9, 27.4, 27.2, 24.9, 24.1, 21.6, 19.4, 12.8$ ; IR (neat):  $\tilde{\nu} = 3421, 2934, 2863, 1739, 1608, 1582, 1509, 1446, 1250, 1175, 1036, 827\text{ cm}^{-1}$ ; HRMS (FAB): calcd for  $\text{C}_{45}\text{H}_{60}\text{O}_4$ : 664.4492 [ $\text{M}-\text{OH}$ ] $^+$ ; found 664.4489.

**24-O-(4,4'-Dimethoxytrityl)cholane-3,24-diol 3-(2-cyanoethyl)-*N,N*-diisopropylphosphoramidite ( $3\alpha,5\beta$ ) (4):** Chloro-(2-cyanoethoxy)-*N,N*-diisopropylaminophosphine (49  $\mu\text{L}$ , 0.23 mmol) was added to a solution of **3** (89 mg, 0.15 mmol) and *N,N*-diisopropylphosphoramidite (DIPEA; 49  $\mu\text{L}$ , 0.23 mmol) in  $\text{CH}_2\text{Cl}_2$  (2 mL). After the reaction mixture had been stirred at room temperature for 15 min, 5%  $\text{NaHCO}_3$  (30 mL) solution and  $\text{CH}_2\text{Cl}_2$  (8 mL) were

added. The organic layer was dried ( $\text{MgSO}_4$ ) and concentrated under reduced pressure. Purification by flash chromatography provided the product as a white solid (69 mg, 0.081 mmol, 54%).  $^1\text{H}$  NMR (300 MHz,  $\text{CDCl}_3$ )  $\delta$  = 7.35 (d,  $J$  = 7.6 Hz, 2H), 7.25–7.11 (m, 7H), 6.73 (d,  $J$  = 8.7 Hz, 4H), 3.70 (s, 9H), 3.54–3.51 (m, 2H), 2.93–2.90 (m, 2H), 2.65 (t,  $J$  = 6.4 Hz, 2H), 1.88–0.80 (m, 46H), 0.53 (s, 3H);  $^{13}\text{C}$  NMR (75.5 MHz,  $\text{CDCl}_3$ )  $\delta$  = 159.0, 146.2, 137.6, 130.7, 129.0, 128.3, 127.2, 113.7, 110.1, 86.4, 77.9, 75.2, 74.9, 64.7, 59.1, 58.8, 57.2, 56.9, 55.9, 43.8, 43.7, 43.4, 43.0, 41.1, 40.9, 36.6, 36.2, 36.0, 35.3, 33.1, 32.3, 30.3, 28.9, 28.0, 27.4, 27.1, 25.4, 25.3, 25.2, 25.1, 24.9, 24.0, 21.5, 21.1, 21.0, 19.4, 12.7;  $^{31}\text{P}$  NMR (121 MHz,  $\text{CDCl}_3$ )  $\delta$  = 148.1, 147.4; IR (neat):  $\tilde{\nu}$  = 3353, 2962, 2935, 2866, 1608, 1509, 1463, 1446, 1376, 1364, 1300, 1250, 1178, 1035, 975, 827, 754  $\text{cm}^{-1}$ ; HRMS (FAB): calcd for  $\text{C}_{54}\text{H}_{78}\text{O}_5\text{N}_2\text{P}_1$ : 865.5648  $[\text{M}+1]^+$ ; found 865.5641.

**Purification of synthesized L-ODNs:** The synthesized oligonucleotides were cleaved from the solid support by treatment with 30% aqueous  $\text{NH}_4\text{OH}$  (1.0 mL) for 10 h at 55°C. The crude products from the automated ODN synthesis were lyophilized and diluted with distilled water (1 mL). The ODNs were purified by HPLC (Merck LichoCART C18 column, 10×250 mm, 10  $\mu\text{m}$ , 100 Å pore size). The HPLC mobile phase was held isocratically for 10 min with 5% acetonitrile/0.1 M triethylammonium acetate (TEAA) buffer solution (pH 7.0) at a flow rate of 3  $\text{mL min}^{-1}$ . The gradient was then increased linearly over 10 min from 5% acetonitrile/0.1 M TEAA to 50% acetonitrile/0.1 M TEAA at the same flow rate. The fractions containing the purified ODN were pooled and lyophilized. 80% aqueous acetic acid was added to the ODN. After 30 min at ambient temperature, the acetic acid was evaporated under reduced pressure. The residue was diluted with water (1 mL), and the solution was purified by HPLC under the conditions described above. The ODNs were analyzed by HPLC to check their purities (Agilent, ZORBAX Eclipse, XDB-C18, 4.6×150 mm, 5  $\mu\text{m}$ ), by using almost the same eluent system, but at a flow rate of 1  $\text{mL min}^{-1}$ .

**Fluorescence detection procedure for the cellular uptake study:** For detection of the cell permeability of synthetic ODNs, we attached FITC (fluorescein) at the 5'-end of  $\text{T}_{12}\text{-L-T}_{12}$  and  $\text{T}_{12}\text{-C}_4\text{-T}_{12}$  as the fluorescence label. The HeLa cells ( $2 \times 10^5$  cells per well) were grown for 24 h on cover slips placed in each well of a 24-well plate at 37°C in a humidified incubator supplemented with 5%  $\text{CO}_2$ . Each nucleotide,  $\text{T}_{12}\text{-L-T}_{12}\text{-FITC}$  or  $\text{T}_{12}\text{-C}_4\text{-T}_{12}\text{-FITC}$ , was diluted in serum-free DMEM (Dulbecco's Modified Eagle Media) at a final concentration of 3.6  $\mu\text{M}$ . The cells were washed with PBS (phosphate-buffered saline), and serum-free media containing each nucleotide (400  $\mu\text{L}$ ) was added to the cells grown on coverslips. After incubation for 8 h, the cells were stained with MitoTracker Red (10  $\text{ng mL}^{-1}$ ; Molecular Probes, Eugene, OR) for 15 min at 37°C. The cells were washed twice with PBS and fixed with 4% formaldehyde for 15 min at room temperature. After being washed twice with PBS, the cells were stained with DAPI (4',6-diamino-2-phenylindole dihydrochloride hydrate; 100  $\mu\text{g mL}^{-1}$ ) for 5 min. The cells were washed twice with PBS, and then the cover slips were air-dried. The cover slips were mounted by using a ProLong Antifade Kit (Molecular Probes) according to the manufacturer's instructions. The fluorescence image was obtained by using either a fluorescence or confocal laser scanning microscope (Axiovert 100 M, Carl Zeiss, Germany).

## Acknowledgements

This work was supported by a KISTEP grant through the NRL (Laboratory for Modified Nucleic Acid Systems) program to B.H.K.

and by the Molecular and Cellular BioDiscovery Research program (M10311000154-03B4500-03110) of the Ministry of Science and Technology to H.J.K. We also thank the BK21 program for partial support.

**Keywords:** DNA structures · oligonucleotides · phosphoramidite

- [1] a) E. Uhlmann, A. Peyman, *Chem. Rev.* **1990**, *90*, 543–584; b) E. T. Kool, *Acc. Chem. Res.* **1998**, *31*, 502–510; c) S. J. Kim, B. H. Kim, *Nucleic Acids Res.* **2003**, *31*, 2725–2734.
- [2] a) A. D. Mesmaeker, R. Haner, P. Martin, H. E. Moser, *Acc. Chem. Res.* **1995**, *28*, 366–374; b) M. Gniadzowski, C. Cera, *Chem. Rev.* **1996**, *96*, 619–634.
- [3] a) J. Wang, *Chem. Eur. J.* **1999**, *5*, 1681–1685; b) D. W. Chen, A. E. Beuscher, R. C. Stevens, P. Wirsching, R. A. Lerner, K. D. Janda, *J. Org. Chem.* **2001**, *66*, 1725–1732.
- [4] M. Takeshita, C.-N. Chang, F. Johnson, S. Will, A. P. Grollman, *J. Biol. Chem.* **1987**, *262*, 10171–10179.
- [5] a) K. Matsuura, T. Yamashita, Y. Igami, N. Kimizuka, *Chem. Commun.* **2003**, 376–377; b) J. Storhoff, C. A. Mirkin, *Chem. Rev.* **1999**, *99*, 1849–1862.
- [6] a) J. L. Staudinger, B. Goodwin, S. A. Jones, D. Hawkins-Brown, K. I. MacKenzie, A. Latour, Y. Liu, C. D. Klaassen, K. K. Brown, J. Reinhard, T. M. Willson, B. H. Koller, S. A. Kliewer, *Proc. Natl. Acad. Sci. USA* **2001**, *98*, 3369–3374; b) J. Sonoda, W. Xie, J. M. Rosenfeld, J. L. Barwick, P. S. Guzelian, R. M. Evans, *Proc. Natl. Acad. Sci. USA* **2002**, *99*, 13801–13803.
- [7] a) D. A. Stetsenko, M. J. Gait, *Bioconjugate Chem.* **2001**, *12*, 576–586; b) H. B. Gamper, M. W. Reed, T. Cox, J. S. Viroso, A. D. Adams, A. A. Gall, J. K. Scholler, R. B. Meyer, *Nucleic Acids Res.* **1993**, *21*, 145–150; c) D. L. Barnard, R. W. Sidwell, W. Xiao, M. R. Player, S. A. Adah, P. F. Tottence, *Antiviral Res.* **1999**, *41*, 119–134; d) R. L. Letsinger, G. Zhang, D. K. Sun, T. Ikeuchi, P. S. Sarin, *Proc. Natl. Acad. Sci. USA* **1989**, *86*, 6553–6556; e) A. S. Boutorin, L. V. Guskova, E. M. Ivanova, N. D. Kobetz, V. F. Zarytova, A. S. Rytte, L. V. Yurchenko, V. V. Vlassov, *FEBS Lett.* **1989**, *254*, 129–132.
- [8] a) I. Toyoaki, I. Teruomi, (Dds Kenkyusho Kk, Japan). *Jpn. Kokai Tokkyo Koho JP-08268917*, **1996**; b) C. S. Ra, S. W. Cho, J. W. Choi, *Bull. Korean Chem. Soc.* **2000**, *21*, 342–344.
- [9] a) S. Wang, A. Friedman, E. T. Kool, *Biochemistry*, **1995**, *34*, 9774–9784; b) E. Azhayaeva, A. Azhayaeva, A. Guzaev, J. Hovinen, H. Lonnberg, *Nucleic Acids Res.* **1995**, *23*, 1170–1176.
- [10] a) F. D. Lewis, S. A. Helvoigt, R. L. Letsinger, *Chem. Commun.* **1999**, 327–328; b) S. J. Kim, B. H. Kim, *Tetrahedron Lett.* **2002**, *43*, 6367–6371; c) F. D. Lewis, T. Wu, X. Liu, R. L. Letsinger, S. R. Greenfield, S. E. Miller, M. R. Wasielewski, *J. Am. Chem. Soc.* **2000**, *122*, 2889–2902; d) F. D. Lewis, R. L. Letsinger, M. R. Wasielewski, *Acc. Chem. Res.* **2001**, *34*, 159–170; e) J. L. Czapinski, T. L. Sheppard, *ChemBioChem* **2004**, *5*, 127–129; f) A. Stutz, S. M. Langenegger, R. Häner, *Helv. Chim. Acta* **2003**, *86*, 3156–3163; g) F. D. Lewis, Y. Wu, L. Zhang, *Chem. Commun.* **2004**, 636–637.
- [11] I. Vargas-Baca, D. Mitra, H. J. Zullyniak, J. Banerjee, H. F. Sleiman, *Angew. Chem.* **2001**, *113*, 4765–4768; *Angew. Chem. Int. Ed.* **2001**, *40*, 4629–4632.
- [12] "Solid-Phase Synthesis of Oligodeoxyribonucleotides by the Phosphotriester Method" M. J. Gait in *Oligonucleotide Synthesis. A Practical Approach*, IRL Press, Oxford, **1984**, pp. 83–115.
- [13] Y. Ueno, M. Takeba, M. Mikawa, A. Matsuda, *J. Org. Chem.* **1999**, *64*, 1211–1217.
- [14] M. Durand, S. Pelouille, N. T. Thuong, J. C. Maurizot, *Biochemistry* **1992**, *31*, 9197–9207.
- [15] a) V. Sklenář, J. Feigon, *Nature* **1990**, *345*, 836–838; b) R. Häner, P. B. Dervan, *Biochemistry* **1990**, *29*, 9761–9765.
- [16] "Circular Dichroism of Biomolecules" A. Rodger, B. Nordén in *Circular Dichroism & Linear Dichroism*, (Eds.: R. G. Compton, S. G. Davies, J. Evans), Oxford University Press, **1997**, pp. 24–29.

Received: May 12, 2004